Hybrid Variational Quantum Circuit for Satellite Image Classification

Trung Thanh Pham*, Loc X. Nguyen†, Phuong-Nam Tran*, Eui-Nam Huh†, Choong Seon Hong†
*Department of Artificial Intelligence, Kyung Hee University, Yongin 17104, Republic of Korea
†Department of Computer Science and Engineering, Kyung Hee University, Yongin 17104, Republic of Korea
Email:{trungpt, xuanloc088, tpnam0901, johnhuh, cshong}@khu.ac.kr

***Abstract*—The requirement for classifying terrain images is increasing with a fast pace due to various important applications such as agriculture, urban planning, and environmental monitoring. Therefore, a variety of pre-trained classification models such as VGG, ResNet, MobileNet, and also Swin-Transformer V2, have been adopted to enhance the accuracy for classifying the satellite images. However, these improvements often come at the cost of increased computational resources, which can be infeasible for edge devices with limited re-training capabilities. In this paper, we integrate the variational quantum circuits into the deep learning model for image classification, which offers superior classification performance with a reduced number of retraining parameters. By utilizing the parameter shift rule, we can compute the gradients of the variational quantum circuit's parameters without relying on traditional backpropagation methods. This characteristic enhances the retraining capabilities of our proposed approach when implemented on edge quantum computers. Despite the limitations posed by Noisy Intermediate-Scale Quantum (NISQ) technology, which restricts the number of qubits available for experimentation, our method effectively combines the advantages of a frozen pretrained SwinV2 encoder with the training efficiency of variational quantum circuits. Therefore, our approach enables us to harness the high accuracy associated with cutting-edge classical deep learning models while simultaneously benefiting from the reduced training parameters characteristic of quantum circuits. Our proposed methodology demonstrates competitive performance, achieving accuracy levels comparable to state-of-the-art classical models on the EuroSAT dataset. Notably, this is accomplished with a significantly lower number of training parameters, highlighting the potential of integrating quantum computing techniques into the domain of image classification.**

***Index Terms*—Satellite image classification, Quantum machine learning, Variational Quantum Circuit.**

This work was supported by the National Research Foundation of Korea(NRF) grant funded by the Korea government(MSIT) (No. RS-2024-00352423) and part by Institute of Information & communications Technology Planning & Evaluation (IITP) grant funded by the Korea government(MSIT) (No.2019-0-01287, Evolvable Deep Learning Model Generation Platform for Edge Computing) and part by IITP(Institute of Information & Coummunications Technology Planning & Evaluation)-ITRC(Information Technology Research Center) grant funded by the Korea government(Ministry of Science and ICT) (IITP-2025-RS-2023-00258649) Dr. CS Hong is the corresponding author.

I. INTRODUCTION

Ground images captured by satellites are essential for a wide array of applications across numerous fields, including agriculture, urban planning, disaster management, and environmental monitoring. These images provide valuable insight that enhances our understanding of land use, vegetation cover, and urban development, making them invaluable for researchers, policymakers, and businesses alike. The ability to analyze and interpret these satellite images enables stakeholders to make informed decisions based on accurate and timely information. One of the most significant advancements in leveraging satellite imagery is terrain satellite image classification, which involves categorizing various land types based on their visual characteristics. This classification process is crucial for applications such as crop monitoring, forest management, and urban expansion analysis, facilitating evidence-based decision-making that can have far-reaching social, economic, and environmental implications [1].

The rapid advancements in deep learning technologies have transformed the landscape of satellite image classification. Convolutional Neural Networks (CNNs) [2] have emerged as powerful tools for this task, with notable architectures such as VGG [3], ResNet [4], MobileNetV2 [5], and transformer-based models like Swin Transformer leading the way [6]. VGG, recognized for its straightforward architecture, employs a series of convolutional layers with small filters, effectively capturing hierarchical features in images. ResNet introduced the innovative concept of residual learning, which enables the training of much deeper networks without encountering issues related to vanishing gradients. This depth allows ResNet to model complex patterns in satellite imagery effectively. MobileNetV2, designed specifically for mobile and edge applications, incorporates depthwise separable convolutions that drastically reduce model size while preserving performance. In contrast, the Swin Transformer utilizes self-attention mechanisms, enabling it to capture complex visual patterns and abstract information of context within images efficiently. The unstructured data pattern representation ability of classical deep learning models is also contributed to by multi-modal LLM advancements [7], [8]. These abstract features are as informative as the original data, even being able to be used as an alternative in data communication [9]. Despite these advancements, a significant trade-off exists between improved accuracy and the computational resources required for training and deploying these models [10]. But the deployment of sophisticated models on edge devices often necessitates substantial processing power, which can limit their practicality in real-world applications where resources are constrained.

As the field of artificial intelligence continues to evolve, the realm of quantum computing has also begun to make notable strides, particularly with the rise of Noisy Intermediate-Scale Quantum (NISQ) technology [11]. Within this context, Variational Quantum Circuits (VQCs) have gained attention as a promising approach for various applications, including image classification [12]. VQCs possess the potential to achieve competitive classification performance while utilizing fewer parameters compared to traditional deep learning models. This efficiency is particularly beneficial in scenarios with limited computational resources, as VQCs can operate effectively on quantum hardware, which may not have the capacity to support large classical models [13].

Gradient-based optimization techniques play a crucial role in the training of VQCs. Among these techniques, finite difference methods and the parameter shift rule are particularly noteworthy [12]. The finite difference method approximates the gradient of a function by evaluating it at slightly perturbed values of the parameters, providing a straightforward means of estimating gradients. On the other hand, the parameter shift rule allows for the computation of gradients directly from the output of the quantum circuit without the need for traditional backpropagation methods. This characteristic is particularly advantageous for VQCs, as it enables the efficient optimization of parameters in environments where conventional optimization techniques may be less effective or impractical.

One of the standout features of VQCs is their ability to maintain classification accuracy with a reduced number of training parameters. This capability is significant for applications where computational resources are limited, such as on edge devices, which are often constrained by power and processing capabilities. By leveraging the inherent efficiency of quantum circuits, researchers can achieve high levels of classification performance while minimizing the computational burden associated with retraining. This dual advantage creates exciting opportunities for deploying advanced image classification methods in real-world scenarios, ensuring that even in resource-limited settings, high-quality analysis remains achievable.

Despite the promising potential of quantum computing, current quantum simulations face significant limitations that restrict the number of qubits available for experiments and influence circuit selection. The Noisy Intermediate-Scale Quantum (NISQ) systems are characterized by their limited qubit counts, typically ranging from a few dozen to a few hundred qubits [14]. This constraint can hinder the complexity of the quantum circuits that can be implemented, as many algorithms and applications require a larger number of qubits to fully realize their potential. Additionally, qubit coherence times and gate fidelity in NISQ devices are often suboptimal, leading to increased noise and errors during computation. These challenges necessitate careful circuit design and selection, as researchers must create models that can operate effectively within these limitations. The ability to scale up quantum circuits and improve error rates is crucial for unlocking the full capabilities of quantum computing, particularly for applications in image classification and other complex tasks.

Looking to the future, the trend of equipping satellites with quantum computing capabilities presents enormous potential for advancing satellite image classification. As quantum technology continues to develop, the prospect of leveraging quantum computing resources within satellite applications could revolutionize how we process and analyze the vast amounts of data captured by modern satellites. The integration of quantum computing into remote sensing technology may lead to enhanced processing speeds and improved accuracy, making it possible to derive more meaningful insights from satellite data that can inform a wide range of applications, from disaster response to climate change monitoring [15]. In summary, our main contributions are as follows:

- We propose a hybrid method that maintains competitive performance while reducing retraining resource requirements. This approach combines classical and quantum techniques, allowing us to achieve high accuracy without the mentioned tradeoff.
- Our approach effectively leverages quantum computing resources in the NISQ era. We optimize our methodology to utilize the limited qubit resources of Noisy Intermediate-Scale Quantum devices. By designing quantum circuits that maintain performance in the presence of constraints, we capitalize on the advantages of quantum computing without relying on fault-tolerant architectures.
- We conduct a wide range of experiments to analyze the classification capabilities of Variational Quantum Circuits. By incorporating a diverse range of classical baseline models in our evaluations, we provide a comprehensive comparison that underscores the strengths of the hybrid variational Quantum Circuits.

II. METHODOLOGY

A. *Background*

Our proposed classification model adopts a hybrid quantum-classical architecture, which is built upon the mathematical principles of quantum mechanics. Specifically, the core of the classifier is a VQC, which requires an understanding of basic quantum information theory and parameterized gate operations.

1) Qubit Notation and State Representation: Qubit is the fundamental component of quantum information. In contrast to classical bit, which exists in a definite state of 0 or 1, a qubit can exist in a superposition of both states. The two computational basis states, $|0\rangle$ and $|1\rangle$, are represented by vectors in the Hilbert space [16]:

$$|0\rangle = \begin{pmatrix} 1 \\ 0 \end{pmatrix}, \quad |1\rangle = \begin{pmatrix} 0 \\ 1 \end{pmatrix}. \tag{1}$$

A general single-qubit state, $|\psi\rangle$, is a linear combination of these basis states:

$$|\psi\rangle = \alpha\,|0\rangle + \beta\,|1\rangle\,, \tag{2}$$

where α and β are complex numbers known as probability amplitudes, satisfying the normalization condition $|\alpha|^2+|\beta|^2 = 1$.

The probability of measuring the state as $|0\rangle$ is $|\alpha|^2$, and the probability of measuring $|1\rangle$ is $|\beta|^2$ [16].

For an n-qubits system, the state space can be represented as the tensor product of n single-qubit spaces, spanning 2^n dimensions. A general n-qubit state $|\Psi\rangle$ is denoted by a vector of 2^n basis amplitudes:

$$|\Psi\rangle = \sum_{x \in \{0,1\}^n} c_x |x\rangle, \quad \text{where} \sum_{x \in \{0,1\}^n} |c_x|^2 = 1, \tag{3}$$

where $|x\rangle$ represents an n-bit binary string.

2) Basic Quantum Gates: Quantum computation is performed by applying unitary operations, known as quantum gates, to the qubit state vectors via matrix multiplication. The following gates are fundamental to constructing VQCs [16].

a) ***Hadamard Gate*** *(H):* The Hadamard gate creates an equal superposition state from a basis state. Its matrix representation is:

$$H = \frac{1}{\sqrt{2}} \begin{pmatrix} 1 & 1 \\ 1 & -1 \end{pmatrix}. \tag{4}$$

b) ***Controlled-NOT Gate*** *(CX **or** $CNOT$):* The CNOT gate is a two-qubit entangling gate, essential for creating quantum entanglement. This gate works with a pair of a control qubit and a target qubit, flipping the target state only if the control qubit is $|1\rangle$. By the nature of 2 qubits input, $CNOT$ gate's matrix representation in the quantum state space is:

$$CX = \begin{pmatrix} 1 & 0 & 0 & 0 \\ 0 & 1 & 0 & 0 \\ 0 & 0 & 0 & 1 \\ 0 & 0 & 1 & 0 \end{pmatrix}. \tag{5}$$

c) ***Rotation Gates*** *(R_x, R_y, R_z):* Parameterized rotation gates are the core building blocks of VQCs, as their rotation angles θ serve as the trainable parameters. They perform a rotation about a specific axis on the Bloch sphere.

$$R_x(\theta) = \begin{pmatrix} \cos(\frac{\theta}{2}) & -i\sin(\frac{\theta}{2}) \\ -i\sin(\frac{\theta}{2}) & \cos(\frac{\theta}{2}) \end{pmatrix}. \tag{6}$$

$$R_y(\theta) = \begin{pmatrix} \cos(\frac{\theta}{2}) & -\sin(\frac{\theta}{2}) \\ \sin(\frac{\theta}{2}) & \cos(\frac{\theta}{2}) \end{pmatrix}. \tag{7}$$

$$R_z(\theta) = \begin{pmatrix} e^{-i\frac{\theta}{2}} & 0 \\ 0 & e^{i\frac{\theta}{2}} \end{pmatrix}. \tag{8}$$

3) Quantum Data Encoding: To use classical data $\mathbf{x} = (x_1, x_2, \ldots, x_M)$ within a quantum circuit, it must first be encoded into the quantum state $|\psi(\mathbf{x})\rangle$. This process, known as quantum embedding, maps the M-dimensional classical feature vector into the 2^n-dimensional Hilbert space.

a) ***Angle Embedding (Parameter Encoding)****:* Angle embedding is a resource-frugal method that maps the classical features directly to the rotation angles of single-qubit gates. For a feature vector $\mathbf{x} = (x_1, \ldots, x_n)$, where n is the number of qubits, the data can be encoded using R_y gates:

$$|\psi(\mathbf{x})\rangle = \left(\bigotimes_{i=1}^{n} R_y(x_i) \right) |0\rangle^{\otimes n}. \tag{9}$$

This encoding is simple to implement and results in shallow circuits, which is advantageous in the NISQ era.

b) ***Amplitude Embedding****:* Amplitude embedding is a dense encoding strategy where the normalized classical features are mapped directly to the amplitudes of the quantum state. To encode a vector $\mathbf{x} \in \mathbb{R}^{2^n}$, the resulting quantum state is:

$$|\psi(\mathbf{x})\rangle = \frac{1}{||\mathbf{x}||} \sum_{i=0}^{2^n-1} x_i |i\rangle. \tag{10}$$

B. *Overall architecture*

The proposed hybrid quantum-classical model integrates a robust pre-trained classical network for feature extraction with a compact VQC as the final classification layer. This architecture is designed to exploit the high accuracy of classical deep learning while minimizing the number of retraining parameters in the final layer.

The overall flow begins with a raw satellite image input x, defined as a three-dimensional tensor of height (H), width (W), and channels (C): $x \in \mathbb{R}^{H \times W \times C}$. The image is first processed by the classical encoder function, $Enc(.)$, which in this work is produced by the frozen weight structure of the Swin Transformer V2. This process extracts a high-level, D-dimensional feature vector V_{enc} from the input image x:

$$V_{enc} = Enc(x), \quad V_{enc} \in \mathbb{R}^D. \tag{11}$$

The resulting high-dimensional classical feature V_{enc} is then prepared for quantum processing. Since the dimension shape of features must align with the number of qubits available, V_{enc} is passed through a classical projection layer, $Proj(.)$, which compresses or adjusts the feature dimension from D to n, the required number of qubits for the VQC. This produces the projected vector V_{proj}:

$$V_{proj} = Proj(V_{enc}), \quad V_{proj} \in \mathbb{R}^n. \tag{12}$$

The projected vector V_{proj} is subsequently used as input for the VQC, which acts as the trainable classification head. The VQC consists of a data encoding block (using V_{proj}) followed by a parameterized Ansatz $U(\theta)$ with trainable parameters θ. The output of the VQC is obtained by measuring the expectation value of an observable operator $\hat{O}$ on the final quantum state, providing a vector of classification scores:

$$VQC(x;\theta) = \langle \hat{O} \rangle = \langle 0| U^\dagger(x,\theta) \hat{O} U(x,\theta) |0\rangle. \tag{13}$$

The core of the hybrid model is the VQC, which acts as a highly expressive, non-linear classifier. For embedding the projected classical feature vector $V_{proj} \in \mathbb{R}^n$ into the quantum state, we utilize the resource-frugal angle embedding strategy. This method ensures minimal circuit depth by mapping each feature component $V_{proj,i}$ directly onto the rotation angle of a single-qubit gate. The Ansatz, or parameterized quantum layer, is built using N layers of the PennyLane Strong Entanglement Circuit. This circuit structure is characterized by alternating layers of single-qubit rotations (which act as trainable parameters) and CNOT entangling layers, which ensure high connectivity and expressive power across all $n = 10$ qubits. Finally, the classification scores are derived by measuring the expectation value of the PauliZ observable across the output qubits. This standard measurement scheme provides

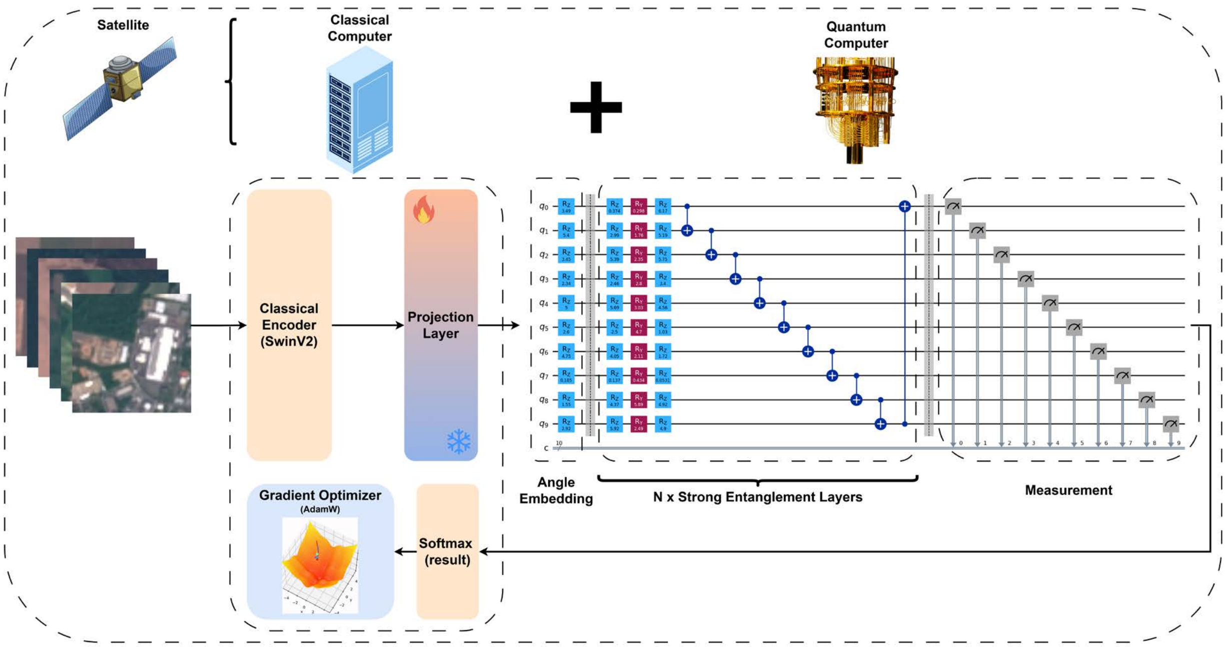

Fig. 1. The overall architecture of the projection layer has two stages of training to take advantage of both classical neural networks and VQCs.

the necessary classical output vector for the final Softmax classification layer.

Finally, the resulting expectation values from the VQC are passed through a classical Softmax activation function, yielding the final probability distribution p over the defined terrain classes:

$$p = \text{Softmax}(VQC(V_{proj}, \theta)). \tag{14}$$

The entire system is trained end-to-end by minimizing a classical loss function the cross-entropy loss through the optimization of the quantum circuit's parameters θ, while the classical encoder's weights remain fixed to ensure resource efficiency during retraining. The cross-entropy loss is shown as follows.

$$\mathcal{L}_{\text{ce}}(p, y) = -\sum_{i=1}^{C} y_i \log(p_i). \tag{15}$$

C. *Two stage training framework*

Due to the limitations of Noisy Intermediate-Scale Quantum (NISQ) devices, particularly the restricted number of qubits (n), the high-dimensional feature vector V_{enc} must be compressed into a lower-dimensional space $V_{proj} \in \mathbb{R}^n$. The classical projection layer $Proj(.)$ optimally maps the complex information from the D-dimensional feature space to n dimensions. The training process consists of two stages to ensure high-quality features for the VQC. The main purpose of the two-stage training is to create a static projection layer without increasing the number of trainable parameters for later retraining on an edge device. In both stages of the training process, the pretrained weights of the classical encoder are frozen and not trained.

1) First Training Stage: In this stage, the weights of the $Proj(.)$ layer are optimized alongside the VQC parameters θ using a subset of the training dataset. The goal is to reduce dimensionality while preserving discriminative information, creating an optimal latent representation V_{proj}.

2) Second Training Stage: This stage focuses on refining the quantum classification head, with the $Proj(.)$ layer's weights frozen. The remaining dataset is used solely to train the VQC parameters θ. This separation allows for efficient learning of non-linear decision boundaries against a stable input, leading to a more stable and accurate final model. After deploying the model to the edge device, only this stage is required for retraining the model. The $Proj(.)$ will act as a static projector function.

III. EXPERIMENTS

A. *Datasets*

The EuroSAT dataset [17] serves as a benchmark for land use and land cover (LULC) classification in remote sensing. It is derived from the Sentinel-2 satellite provided by the Copernicus Earth observation program. The dataset is comprised of **27,000** labeled and geo-referenced image patches, each 64×64 pixels in size. The dataset is categorized into **10 classes**, which include: AnnualCrop, Forest, HerbaceousVegetation, Highway, Industrial, Pasture, PermanentCrop, Residential, River, and SeaLake. The balanced nature and high-resolution multi-spectral data of EuroSAT make it an ideal and rigorous benchmark for evaluating the performance of deep learning and hybrid quantum-classical classification models.

B. *Experiment setup*

The experiments were executed on a high-performance Ubuntu server environment, utilizing an NVIDIA H100 GPU for all classical deep learning and simulation tasks, providing the necessary computational speed for training and evaluation. For the quantum circuit simulation and gradient computation, the **PennyLane** [18] quantum computing framework was employed. The classical encoder component, the Swin Transformer V2, was initialized using pretrained weights from the Base version **SwinV2-B** [6], with these weights subsequently frozen to maintain feature quality and reduce the retraining cost. For rigorous evaluation, the full dataset was split into a $\mathbf{70}\%$ training set, a $\mathbf{15}\%$ validation set, and a $\mathbf{15}\%$ testing set. The model optimization was carried out using the AdamW optimizer [19] with a fixed learning rate of $\mathbf{0.0001}$. The total training process spanned **10 epochs**, leveraging a batch size of **64**. Consistent with constraints on current NISQ hardware, the VQC was implemented using $\mathbf{n = 10}$ **qubits**. The number of Strong Entanglement Layers we use in the VQC is $N = 5$.

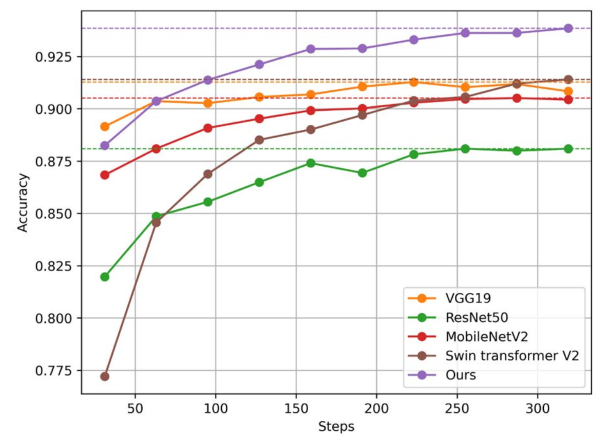

Fig. 2. Validation accuracy diagram

C. Experiment result

For comprehensive comparison, our experiments evaluated the performance of the proposed hybrid quantum-classical model against several established classical architectures: fine-tuned VGG19, ResNet50, MobileNetV2, and SwinV2-B on the EuroSAT dataset [17]. Despite operating with a significantly lower count of trainable parameters in its final classification layer, as detailed in Table III-C, the hybrid approach achieved a competitive result compared to the fully classical models. Specifically, our hybrid VQC model demonstrated a test accuracy of 0.93654. This result is notably competitive when compared to the test accuracies of the pure classical models, which achieved 0.917289, 0.88148, 0.9037, and 0.91975 for VGG19, ResNet50, MobileNetV2, and SwinV2-B, respectively. Furthermore, the robust performance extends to the validation dataset, where the hybrid quantum model achieved the highest validation accuracy of 0.93852. This result surpasses the validation accuracies of the classical counterparts, the detailed validation accuracy shown in Fig. 2. These findings collectively demonstrate a robust improvement in both classification accuracy and the efficiency of the retraining process, affirming the potential of our proposed hybrid architecture. The hybrid VQC model requires only 150 trainable parameters for retraining, representing a significant reduction compared to the classical models.

TABLE I
NUMBER OF TRAINABLE PARAMETERS REQUIRED FOR RE-TRAINING

Model	# Trainable parameters
VGG19	3,212,682
ResNet50	263,562
MobileNetV2	656,778
SwinV2-B	132,490
Hybrid VQC	**150**

IV. CONCLUSION

In this paper, we propose a hybrid variational quantum circuit model for satellite image classification, effectively integrating classical deep learning techniques with quantum computing principles. Our approach leverages the strengths of pretrained models, specifically the Swin Transformer V2, and combines them with the efficiency of VQCs. The results demonstrated competitive classification performance on the EuroSAT, achieving accuracies surpassing state-of-the-art classical models while significantly reducing the number of retraining parameters. This research highlights the potential of quantum machine learning in enhancing image classification capabilities, particularly in resource-constrained environments, and paves the way for future explorations into the integration of quantum computing in remote sensing applications.

REFERENCES

[1] A. A. Adegun, S. Viriri, and J.-R. Tapamo, "Review of deep learning methods for remote sensing satellite images classification: experimental survey and comparative analysis," *Journal of Big Data*, vol. 10, no. 1, p. 93, 2023.

[2] Y. LeCun, L. Bottou, Y. Bengio, and P. Haffner, "Gradient-based learning applied to document recognition," *Proceedings of the IEEE*, vol. 86, no. 11, pp. 2278–2324, 2002.

[3] K. Simonyan and A. Zisserman, "Very deep convolutional networks for large-scale image recognition," in *3rd International Conference on Learning Representations, ICLR, San Diego, CA, USA*, May 2015.

[4] K. He, X. Zhang, S. Ren, and J. Sun, "Deep residual learning for image recognition," in *Proceedings of the IEEE conference on computer vision and pattern recognition*, 2016, pp. 770–778.

[5] M. Sandler, A. Howard, M. Zhu, A. Zhmoginov, and L.-C. Chen, "Mobilenetv2: Inverted residuals and linear bottlenecks," in *Proc. of the IEEE Comput. Soc. Conf. Comput. Vis. Pattern Recognit.*, 2018.

[6] Z. Liu, H. Hu, Y. Lin, Z. Yao, Z. Xie, Y. Wei, J. Ning, Y. Cao, Z. Zhang, L. Dong *et al.*, "Swin transformer v2: Scaling up capacity and resolution," in *Proceedings of the IEEE/CVF conference on computer vision and pattern recognition*, 2022, pp. 12 009–12 019.

[7] Y. Qiao, P.-N. Tran, J. Yoon *et al.*, "Deepseek-inspired exploration of rl-based llms and synergy with wireless networks: A survey," *ACM Comput. Surv.*, Early Access, Nov. 2025.

[8] Y. Qiao *et al.*, "Towards artificial general or personalized intelligence? a survey on foundation models for personalized federated intelligence," *ArXiv:2505.06907*, 2025.

[9] L. X. Nguyen *et al.*, "A contemporary survey on semantic communications: Theory of mind, generative ai, and deep joint source-channel coding," *IEEE Commun. Surveys Tuts.*, Early Access, 2025.

[10] H.-I. Liu, M. Galindo, H. Xie, L.-K. Wong, H.-H. Shuai, Y.-H. Li, and W.-H. Cheng, "Lightweight deep learning for resource-constrained environments: A survey," *ACM Computing Surveys*, vol. 56, no. 10, pp. 1–42, 2024.

[11] X. Pan, Z. Lu, W. Wang, Z. Hua, Y. Xu, W. Li, W. Cai, X. Li, H. Wang, Y.-P. Song *et al.*, "Deep quantum neural networks on a superconducting processor," *Nature Communications*, vol. 14, no. 1, p. 4006, 2023.

[12] M. Cerezo, A. Arrasmith, R. Babbush, S. C. Benjamin, S. Endo, K. Fujii, J. R. McClean, K. Mitarai, X. Yuan, L. Cincio *et al.*, "Variational quantum algorithms," *Nature Reviews Physics*, vol. 3, no. 9, pp. 625–644, 2021.

[13] A. Abbas, D. Sutter, C. Zoufal, A. Lucchi, A. Figalli, and S. Woerner, "The power of quantum neural networks," *Nature Computational Science*, vol. 1, no. 6, pp. 403–409, 2021.

[14] Y. Zhao, Y. Chen, H. Li, Y. Wang, K. Chang, B. Wang, B. Li, and Y. Han, "Full state quantum circuit simulation beyond memory limit," in *2023 IEEE/ACM International Conference on Computer Aided Design (ICCAD)*. IEEE, 2023, pp. 1–9.

[15] S. Rainjonneau, I. Tokarev, S. Iudin, S. Rayaprolu, K. Pinto, D. Lemtiuzhnikova, M. Koblan, E. Barashov, M. Kordzanganeh, M. Pflitsch *et al.*, "Quantum algorithms applied to satellite mission planning for earth observation," *IEEE J. Sel. Top. Appl. Earth Obs. Remote Sens.*, vol. 16, pp. 7062–7075, 2023.

[16] Y. Du, X. Wang, N. Guo, Z. Yu, Y. Qian, K. Zhang, M.-H. Hsieh, P. Rebentrost, and D. Tao, "Quantum machine learning: A hands-on tutorial for machine learning practitioners and researchers," *ArXiv:2502.01146*, 2025.

[17] P. Helber, B. Bischke, A. Dengel, and D. Borth, "Eurosat: A novel dataset and deep learning benchmark for land use and land cover classification," *IEEE Journal of Selected Topics in Applied Earth Observations and Remote Sensing*, vol. 12, no. 7, pp. 2217–2226, 2019.

[18] V. Bergholm, J. Izaac, M. Schuld, C. Gogolin, S. Ahmed *et al.*, "Pennylane: Automatic differentiation of hybrid quantum-classical computations," 2022. [Online]. Available: https://arxiv.org/abs/1811.04968

[19] I. Loshchilov and F. Hutter, "Decoupled weight decay regularization," in *Proc. International Conference on Learning Representations (ICLR)*, May 2019.